ORIGINAL ARTICLE

A C G publications *Bioorg. Med. Chem. Rep.* X:X (202X) X-X

Bioorganic & Medicinal Chemistry Reports

The anti-pathogenic activity and DNA gyrase inhibition of freshwater crabs (*Barytelphusa cunicularis*) are related to their structure-activity relationship

Sanjay Chavan[1*], Anil G. Beldar[2] and Rekha B. More[3]

[1]*Department of Chemistry, Rani Laxmibai Mahavidyalaya, Parola, Dist. Jalgaon, 425111, MS, India.*
[2]*Department of Chemistry, PSGVPM's ASC College, Shahada, Dist. Nandurbar, 425409, MS, India*
[3]*Department of Chemistry, Shri Swami Shatkooacharyaji Maharaj ASC College, Saikheda. Tal. Niphad, Dist. Nashik, 422210, MS, India*

(Received May 5, 2024; Revised July 22, 2024; Accepted July 26, 2024)

Abstract: For screening purposes, there has been interest in creating natural product scaffolds that closely resemble drug-like compounds utilizing combinatorial chemical approaches. Various screening techniques are being developed to improve the data mining and drug development campaigns' usage of natural materials. From the tissue extract of the freshwater crab Barytelphusa cunicularis, four chemicals were shown to have biological activity against both gram-positive and gram-negative bacteria, including E. coli and B. subtilis, and S. aureus. Four pathogens were used in this study: *A. niger, M. furfur, A. flavus,* and *P. Chrysosporium.* Flavus and P. Chrysosporium, but poorly against *A. Niger* and *M. Furfur.* To further the development of potential therapeutics, structure-activity relationship (SAR) analysis via a virtual screening protocol was conducted. Bioactivity assessments confirmed the compounds' efficacy against both bacterial and fungal targets. Molecular docking analyses revealed that all four organic compounds exhibit favorable absorption, distribution, metabolism, excretion, and toxicity (ADME/T) properties and bind with the protein DNA gyrase at diverse sites. In conclusion, the compounds' notable activity with DNA gyrase suggests their potential for drug design exploration.

Keywords: Combinatorial; *Barytelphus cunicularis*; bacteria, molecular docking; ADME/T; DNA gyrase; SAR.

1. Introduction

The primary responsibility of natural product processing is drug development, which is also the researcher's ultimate goal. All that remains of the separated component is a lead compound, and it is the ideal medication for the intended illnesses. Therefore, processing natural products (i.e., extraction, isolation, and structural elucidation) alone is insufficient to fully produce a medication[1]. When researchers follow the natural product processing protocol, which includes extraction, isolation, structure elucidation, and computational investigation, a drug will eventually be developed.

* Corresponding author: E-Mail: sanjayvchavan48@gmail.com; Phone: + 919922085588

The article was published by ACG Publications
http://www.acgpubs.org/journal/organic-communications © Month-Month 202X EISSN:1307-6175
DOI: http://doi.org/10.25135/acg.oc.34.2405.3223
Available online: September 11, 2024

Computational methods are a key tool in drug creation. Molecular docking and SAR techniques are frequently employed in the virtual screening of massive databases to help choose a molecule and anticipate protein-ligand interactions. With multiple successes in discovering novel lead compounds for pharmaceutical development, virtual screening is fast becoming the major use of computational docking approaches [2–5]. The campaign's virtual screening methodology is outlined. In specifics, we did the following: (i) arrange the bioactive compounds that we isolated from *Barytelphusa Cunicularis* tissue; (ii) prepare libraries of analogues that are similar to the bioactive compounds; (iii) perform a 3D pharmacophoric scan; (ii) use molecular docking to assess the binding mode of all retrieved compounds using the 3D structure of the ligand DNA gyrase crystal structure. (iv) *in-silico* ADME parameters using QikProp to find the potent bioactive compounds; (iii) compounds that exhibit the most notable docking score against the crystal structure of DNA gyrase have been further filtered using Lipinski's rule of five to assess drug likeness, which becomes an essential tool to facilitate drug discovery. One of the main causes of morbidity and mortality in humans is infection. The quick bacterial adaptation to antibiotics, which leads to the development of resistance when antibacterial medications are introduced into clinical usage, is the primary cause of the pharmaceutical industry's inability to meet the growing need for efficacious innovative antibacterial drugs[6]. The World Health Organization has identified antibiotic resistance as one of the biggest hazards to public health worldwide. Antibiotic resistance is predicted to be the cause of 10 million annual deaths after 25 years, hence appropriate action must be taken to halt this harmful trend. Roughly half of the antibiotics administered for treating human illnesses have been shown to be unneeded[7].

The development of new antibacterial drugs should focus on two crucial bacterial enzymes: DNA gyrase and topoisomerase II. The development of novel antibiotics and boosting the effectiveness of medications that are now undergoing clinical trials are crucial tactics in the battle against antibiotic resistance. Because of their various biological and industrial uses, including as enzyme inhibitors, chelating agents, antibacterial agents, and anticancer agents, isolated compounds attracted a lot of attention from the pharmaceutical industry in this context and were considered attractive candidates for additional drug development[8-10]. This has been done as a part of our continuing programmed to create new antifungal and antibacterial medicines based on four compounds that have been isolated from *Barytelphusa Cunicularis* tissues. According to our report, a new class of drugs with strong antibacterial action has been introduced as unique bioactive compounds[11]. These findings encouraged us to investigate and assess their antibacterial activity further in order to comprehend the mechanism of action of the active ingredients. One such method is the measurement of DNA gyrase binding affinity as a possible inhibitor[12]. To choose the most promising inhibitor or inhibitors for additional lead optimization, a molecular docking technique will also be used. To further design novel compounds that target DNA gyrase and are effective against resistant microbial strains like amphotericin-B-resistant pathogens and chloramphenicol, the most potent inhibitor will be identified through the investigation of structure-activity relationships, or SARs. Here, we report the process of attaching to and stabilizing DNA cleavage complexes to identify bacterial DNA gyrase inhibitors[13].

2. Experimental

2.1. General Procedures

Melting points were not recorded in open glass capillaries. UV-visible spectra on Shimadzu and the IR spectra were recorded on an ATR Bruker alpha FT-IR spectrophotometer (R. C. Patel College, Shirpur, India). NCHS analyses were carried out by Thermo Finnigan calibrated by the K-factor method (Punjab University, Chandigarh, India), 13C NMR and 1H NMR spectra were recorded on 500.13 MHz by a Brucker spectrophotometer (SSPU Pune, India), and LC-MS were checked by Wockhart R & D Lab, Aurangabad, India, Single Crystal Instrument. Model: X-ray wavelength: Mo, x-cen: 390.4189, y-cen: 185.8663, distance: 51.0000, beam: -0.0435 (Model Interpol. in use), University of Hyderabad, India. The interpretation of all the spectral data of the isolated compounds was anticipated from the reference books and table charts on the Sigma-Aldrich website. Four bacterial and four fungus strains were selected for this study, namely, bacteria are Staphylococcus aureus, Bacillus subtilis, Escherichia coli, and Proteus vulgaris, while fungus is Aspergillus niger, Candida albicans, Aspergillus flavus, and Phanerochaete chrysosporium.

A total of eight pathogens were obtained from the National Collection of Industrial Microorganisms, National Chemical Laboratory (NCL), Pune, 411008, India.

2.2. Culture Method

The 6 mm disc, often known as the disc diffusion method or agar diffusion experiment, was employed in this investigation. The susceptibility test strategy was used for studies of bacteria using disc diffusion and dilution procedures and for studies of fungal species using yeast and the filamentous method. The National Collection of Industrial Microorganisms (NCIM) at the National Chemical Laboratory (NCL), Pune 411008 [India] provided the strains of bacteria *Staphylococcus aureus* (NCIM 2079), *Bacillus subtilis* (NCIM 2063), *Escherichia coli* (NCIM 2109), *Proteus vulgaris* (NCIM 2172), and fungal strains *Aspergillus niger* (NCIM 545), *Malassezia furfur* (NCIM 3471), *Aspergillus flavus* (NCIM 650), and *Phanerochaete chrysosporium* (NCIM-1106).

2.2.1. Concentration of Compounds

The concentration of each compound's stock solution (1000 micrograms per millilitre) was made using DMSO solvent. One hundred micrograms of concentration were used for each disc in the assay. High-media antibiotic disc: As a benchmark, 10 micrograms of chloramphenicol per disc are moistened with water.

2.2.2. Media Used

Microbiological mediums for fungus and bacteria and Hi-Media agars were used under particular circumstances. The composition of nutrient agar (Hi-media) for bacteria (gL-1): sodium chloride: 5.0, beef extract: 10.0, peptone: 10.0 (PH: 7.2), potato dextrose agar: 200, dextrose: 20, and agar: 15 for fungus (all components of Hi-media). At 250 °C, the final PH was 5.6 ± 0.2.

2.3. Theoretical Prediction of Pharmacokinetics or ADME/T Parameters

To prevent wasting time and resources, it is imperative to assess the ADME/T characteristics of the above-mentioned substances. Thus, we used Swiss ADME to estimate the ADMET properties of the synthetic drugs that we designed. The "Rule of Five," or four ADMET characteristics, was proposed in order to classify these compounds as the best compounds. The most reliable and well-known rule-based drug-likeness filter, known as the rule of five, is used to determine if a substance is well absorbed when taken orally. The five rules comprise:

1) Molecular weight (MW)≤ 500;
2) Octanol/water partition coefficient (iLOGP = A log P) ≤ 5;
3) Number of hydrogen bond donors (HBDs) ≤ 5; and
4) Number of hydrogen bond acceptors (HBAs) ≤ 10.6.

The QED method, also known as the quantitative estimate of drug-likeness, produced eight physio-chemical properties. These properties comprised the above-mentioned four rules of five and four additional rules, which are as follows: 1) molecular polar surface area (TPSA); 2) number of rotatable bonds (ROTBs); 3) number of aromatic rings (nAROMs); and 4) number of alerts for undesirable sub-structures (ALERTs, such as PAINS #alert and Brenk #alert). The ADMET properties were developed, and the Swiss ADME drug design study was conducted.

3. Results and Discussion

3.1. Chemistry of Isolated Compounds

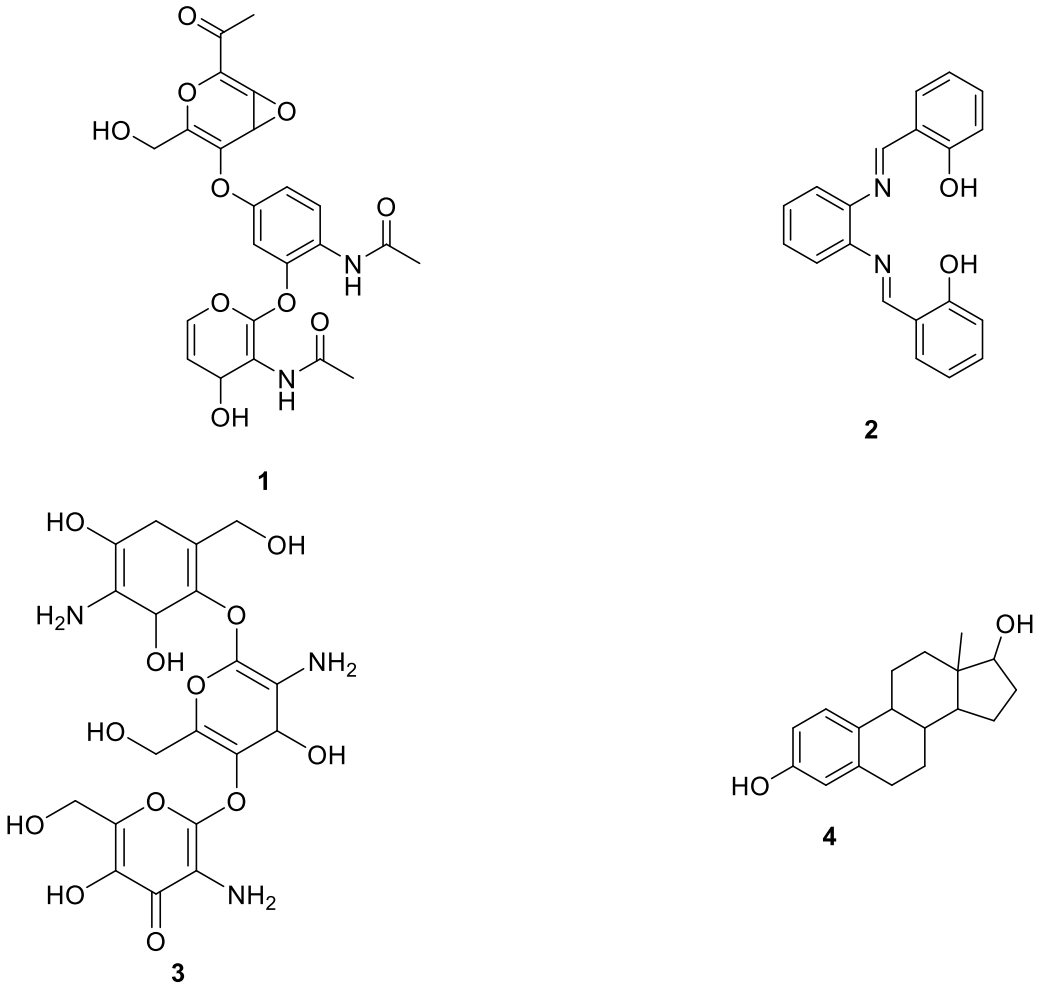

Figure 1. Structures of isolated compounds from tissue of **B**. *Cunicularis*

Using column chromatography, the ethanol extract was observed by increasing polarity. The fractions were labelled after they were collected and then subjected to TLC analysis again using different ratios based on the final solvent system. Out of those, four single compounds were visualized: one spot in P.E.: E.A. (8.5:1.5), one spot in PE: EA: Et. (9.5:0.5:0.5), and two spots in P.E.: E.A.: Et. (7.5:2.0:0.5). When the purity level of these four fractions was examined using HPLC analysis, it was discovered that each fraction had a minor amount of contaminants. The separated organic compounds were dried, and then they were placed in a sample vial for additional analysis using mass, UV, IR, ^{1}HNMR, and ^{13}CNMR spectroscopy (Figure1).

3.2. Spectral Data of Isolated Compounds

*Compound **1**:* UV; 771.50 nm at 0.0022 abs, 322.00 nm at 0.5889 abs, 308.50 nm at 0.3983 abs, 253.00 nm at 0.1664 abs, 212.00 nm at 0.1396 abs; FTIR *:*Aromatic ring (3-Peaks): 1460.16 cm^{-1}, 1535.39 cm^{-1} and 1648.23 cm^{-1}, Ar-OH: 634.01 to 3580.97 cm^{-1}, stretching of N-H: 2954.08 cm^{-1} to 2850.88 cm^{-1},

conjugated ketone C=O: 1710.92 cm^{-1}, strong C-O stretching aromatic ester: 1260.52 to 1311.64 cm^{-1}, aromatic compound C-H bending 2016.92 cm^{-1} weak overtone, 1116.82 to1081.44 cm^{-1} strong C-O stretching secondary alcohol. ^{1}H NMR (400 MHz, DMSO-d^6, δ ppm): 7.86-6.84 (m, 6H, Ar-H); 2.51-2.50 (s, 2H, -NH); 8.26-8.23 (s, 1H, -OH); 1.62 (s, 3H, Ar-CO-R); 1.08-1.05 (s, 6H, -NH-CO-CH_3); 3.39 (s, 2H, CH_2); ^{13}C NMR (400 MHz, DMSO-d^6, δ ppm) :19.05, 26.31, 39.38, 39.59, 40.02, 40.44, 40.65, 56.50, 127.46, 128.45, 129.29, 131.28 and 175.66; *LC-MS:* LC-MS (ES+, 8.78e4): *m/z* = 485.40 (M+) for $C_{23}H_{22}N_2O_{10}$.

*Compound **2**:* UV: 472.50 nm at 0.0369 abs, 444.50 nm at 0.0451 abs, 418.00 nm at 0.0411 abs, 268.00 nm at 1.7683 abs, 243.00 nm at 2.4791 abs; FTIR : Aromatic ring: 1370.16 cm^{-1}, and 1639.55 cm^{-1}, Ar-OH: 3523.10 to 3419.90 cm^{-1}, stretching of -C=N: 2105-37 cm^{-1}, aromatic compound =C-H bending 2852.81 cm^{-1} weak overtone; ^{1}H NMR (500 MHz, DMSO d^6, δ ppm) : 7.97-6.61 (m, 12H, Ar-H), 2.64-2.51 (s, 2H, -HC=N), 3.34 (s, 2H, -OH); ^{13}C NMR (400 MHz, DMSO-d^6, δ ppm) : 39.41, 39.62, 39.83, 40.04, 40.24, 40.46, 40.67, 136.19, 151.30 and 170.96; *LC-MS* :LC-MS (ES+, 8.78e4): *m/z* = 316 (M^+) for $C_{20}H_{16}N_2O_2$

Compound 3: UV *:*470.50 nm at 0.0138 abs, 440.50 nm at 0.0167 abs, 418.50 nm at 0.0161 abs, 271.50 nm at 2.4108 abs, 241.50 nm at 1.9462 abs; FTIR: -NH_2: 3581.93 cm^{-1} to 3414.12 cm^{-1}, aromatic ring: 1461.13 cm^{-1}, 1535.39 cm^{-1} and 1680.05 cm^{-1}, Ar-OH: 3790.25 cm^{-1} to 3735.28 cm^{-1}, carbonyl carbon -C =O: 1767.82 cm^{-1}, -CH_2: 1369.50 cm^{-1}, Ar-O-Ar: 1260.52 cm^{-1}; ^{1}H NMR (500.13 MHz, $CDCl_3$, δ ppm): 7.69-6.96 (m, 5H, Ar-H), 3.35-2.51 (s, 6H, -NH_2), 8.95 (s, 3H, -OH), 12.94 (s, 3H, COOH); ^{13}C NMR (500 MHz, DMSO-d_6, δ ppm): 39.41, 39.62, 39.84, 40.05, 40.47, 40.68, 117.16, 119.57, 120.25, 128.28, 132.93, 133.93, 142.76, 160.86 and 164.52; LC-MS: LC-MS (ES+, 8.78e4): *m/z* = 485 (M^+) for $C_{19}H_{23}N_3O_{12}$.

*Compound **4**:* UV: 769.50 nm at -0.0002 abs, 648.00 nm at 0.0130 abs, 503.00 nm at 0.0048 abs, 487.00 nm at 0.0055 abs, 319.50 nm at 1.0670 abs, 306.00 nm at 0.1890 abs, 270.50 nm at 0.1016 abs, 265.00 nm at 0.0981 abs, 246.00 nm at 0.0825 abs; FTIR: Aromatic ring: 1658.48 cm^{-1} and 1543.10 cm^{-1}, Ar-OH: 3447.87 cm^{-1}, -CH_2: 1218.09 cm^{-1}, -C-H stretching: 2923.22 cm^{-1} to 2851.85 cm^{-1}; ^{1}H NMR of S4 (500.13 MHz, $CDCl_3$, δ ppm): 7.84-6.53 (m, 3H, Ar-H), 9.77 (s, 2H, -NH_2), 10.03-8.50 (s, 2H, -OH), 3.34 (d, 6H -CH_2-C), 2.51 (s, 3H, -CH_3); ^{13}C NMR (500 MHz, DMSO-d_6, δ ppm): 39.41, 39.62, 40.04, 40.46, 40.67, 114.90, 116.03, 116.72, 127.22, 128.57, 130.94, 136.53, 143.92, 156.75 and 160.71; LC-MS: LC-MS (ES+, 8.78e4): *m/z* = 272 (M^+) for $C_{18}H_{24}O_2$

3.3. Microbial Activity

The crude freshwater crab tissue extract showed the highest inhibition zones of 15.31 mm and 11.99 mm against *S. aureus* and *E. coli*, respectively, while a moderate inhibition zone against *B. subtilis* and *P. vulgaris* (Figure 2).

Table 1. Antibacterial activity data crab tissue extract*

Name of the Organism	positive control inhibition zone	Inhibition Zone
E.coli	25.9	12.0
P. vulgaris	22.4	8.5
S.aureus	15.3	15.3
B. subtilis	22.9	8.9

*Chlorapmhenicol used as positive control

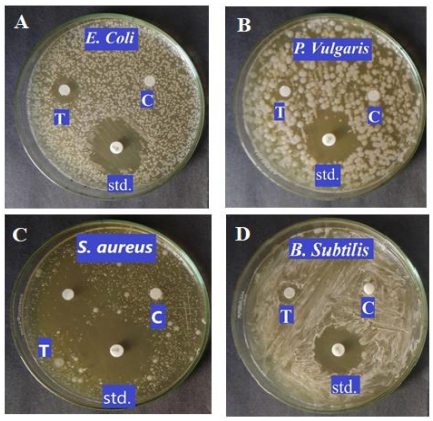

Figure 2. Antibacterial activity against human pathogens

Animals are rich sources of bioactive compounds and most of the compounds are derived from marine biota, but structure determination, synthesis and bioactivities are big problems[12]. Most of the marine animals set toward the drug discovery due to their clinical potential[13]. This area is maximum focused for research in many disciplines like chemistry, biology, biochemistry and biotechnology. The bioactive compounds shown by many marine crustains for gram positive and gram-negative bacteria so many researchers published the antimicrobial activity[14]. The peptides are isolated from many crab species and showed antifungal activity against the human pathogens, so many compounds are exploring drug development[15]. In this research the antimicrobial activity of the crude extract from tissue of *Barytelphusa Cunicularis* was studied against human pathogens toward different organisms. In this study bacterial strain are used, the bacteria differed gram positive and gram-negative bacteria were utilized for this examination purpose, the *E. Coli* and *P. Vulgaris are* gram negative while *S. Aureus* and *B. Subtilis* are gram positive bacteria, out of these bacterial strains the crude tissue extract showed 1.31 mm inhibition zone against *S. Aureus* while inhibition zone against the *E. Coli* showed 11.99 mm, so crab tissue extract showed strong activity these organisms. The gram-positive bacteria *B. Subtilis* showed 8.97 mm inhibition zone and gram-negative bacteria *P. Vulgaris* showed 8.52 mm inhibition zone toward the extract; it means that the extract showed weak activity towards these organisms.

From the present study, we concluded that freshwater crab tissue showed significant activity against the pathogen, indicating the presence of most bioactive compounds which can be explored for drug development. The selected microorganisms can be focused on the biosynthetic genes and volatile compounds confirmed their potential to utilize an able source of antimicrobial drug, further study yet requires to finish the development of natural potent drugs in pharmaceutical research.

3.4. ADMET properties

Table 2. Calculated ADMET parameters of the designed compounds.

Compound No	Mol Wt. g/mol	HBA	HBD	TPSA	iLOGP	Class	Log kP cm/s	Lipinski	PAINS	Synthetic accessibility	BRENK
1	484.46	9	3	144.95	0.00	Soluble	-9.27	Yes	0	5.23	1
2	316.35	4	2	65.18	2.36	Soluble	-5.37	Yes	0	2.81	1
3	272.38	2	2	40.46	2.58	Soluble	-5.11	Yes	0	3.49	0
4	484.43	13	9	257.34	0.00	Soluble	-12.26	Yes	0	6.11	0

According to Lipinski's rule of five and the concept of QED as presented in Table 2, all the isolated compounds follow the Lipinski and QED rules and all the MW, RB, HBD, HBA, TPSA, iLOGP, are within the acceptable range. Also, there is no alert for PAINS and 2 Brenk for compounds 1 and 2, which indicates that the compounds are quite specific. Hence, these isolated compounds are the most active anti-bacterial and anti-fungal compounds and possess good pharmacokinetic properties[16-18].

3.5. Molecular Docking Study

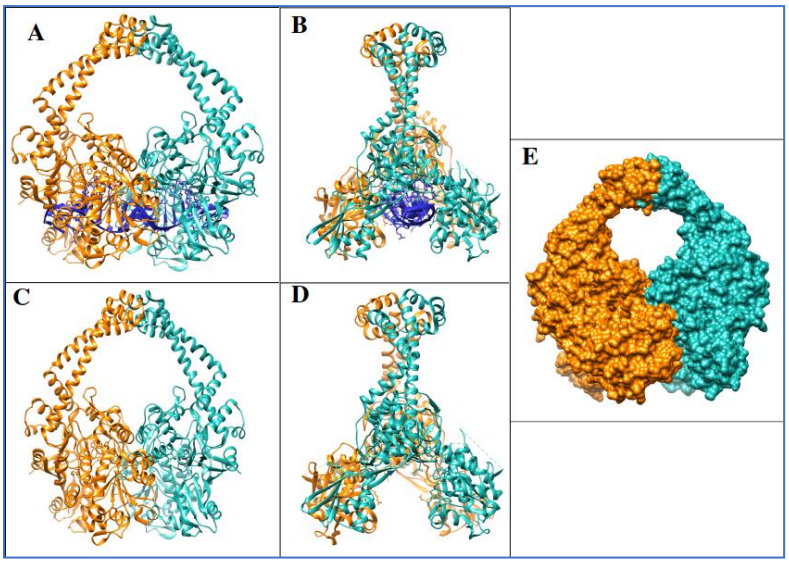

Figure 3. Structure of DNA gyrase receptor. Here the structure (A) shows the DNA gyrase with DNA and (B) side view of the same structure of DNA gyrase. (C) Structure of DNA gyrase without DNA double-helical strand which is further used for molecular docking study and (D) side view of the DNA gyrase without DNA strand and (E) Solvent accessible surface of the DNA gyrase structure.

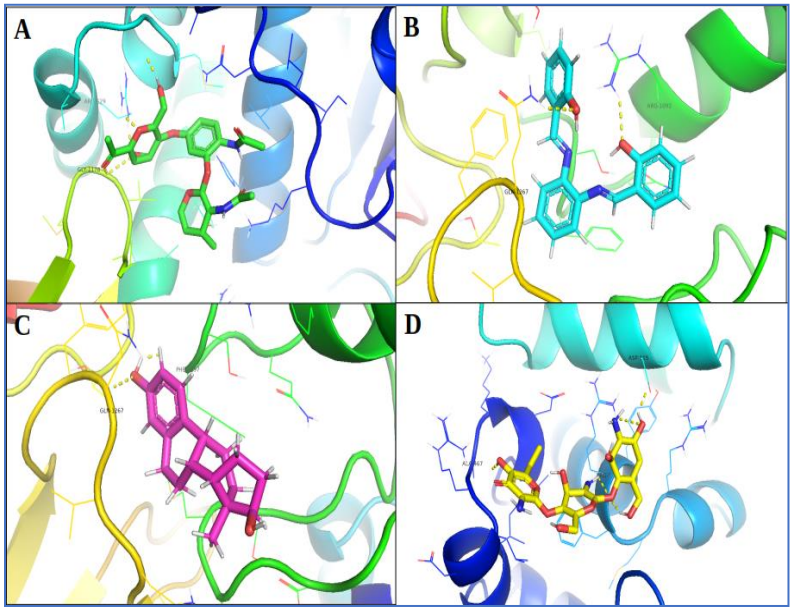

Figure 4. Binding mode of potential antibacterial compounds with DNA gyrase (A) Showing the DNA gyrase with compound 1 (green), (B) Show the DNA gyrase with compound 2 (cyan), (C) Show the DNA gyrase with compound 3 (magenta), (D) Shows the DNA gyrase with compound 4 (yellow)

We employed topoisomerase II, also known as DNA gyrase, to investigate the binding mechanism of our several synthetic therapeutic compounds against the target protein of the bacterial system. A promising target to investigate the binding mechanism of recently isolated medicinal compounds was previously the DNA gyrase. Moreover, amphotericin B and chloramphenicol were employed as control medications in order to comprehend the anti-fungal and anti-bacterial agents. Topoisomerase II DNA gyrase is a significant target enzyme and one of the classes of enzyme inhibitors that have been studied the most[19-23].

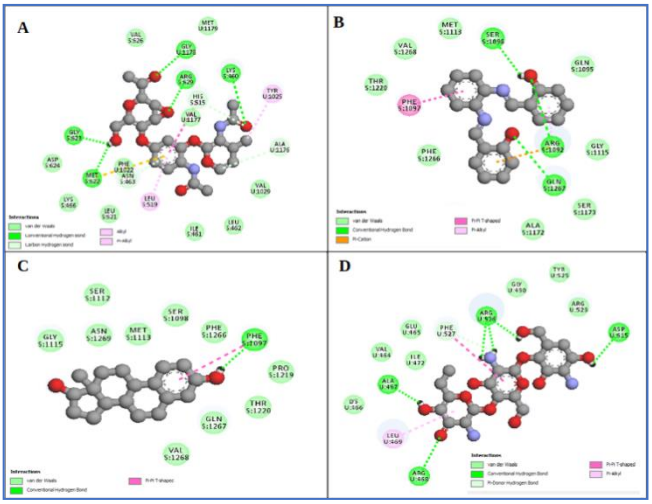

Figure 5. Two-dimensional interactions of antibacterial compounds with DNA gyrase receptor (A) 2D interactions of DNA gyrase residues with compound 1 (B) 2D interactions of DNA gyrase residues with compound 2 (C) 2D interactions of DNA gyrase residues with compound 3 and (D) 2D interactions of DNA gyrase residues with compound 4. Here, the color code of type interactions such as classical hydrogen bonding, Pi type, van der Waals, etc., are given in each column (A), (B), (C) and (D).

Table 3. Bonding interaction of various antibacterial drug compounds with DNA gyrase receptor

Protein	Binding energy Kcal/mol	Atoms involved in the interaction	Distance (Å)	Angle (°)	Figure Ref.
1	-7.09	LYS460:HZ1 - :UNL1:O	2.98476	118.996	6A
		ARG517:HE- GLU1017:OE2	2.43747	122.335	
		ARG629:HE - :UNL1:O	1.88311	154.119	
		ARG1012:HN1 - GLN605:O	2.26039	123.973	
		ILE1014:HN - LYS607:O	2.56727	141.03	
		LEU1430:HN - LEU1426:O	2.96046	106.893	
		LEU1430:HN - MET1428:O	2.4405	139.718	
		ARG1431:HN - LEU1426:O	2.07249	153.717	
		GLY1435:HN - SER1401:O	2.33415	135.765	
		LEU1436:HN - ASP1402:O	1.77206	151.67	
		ARG1438:HH21- ARG1399:O	2.4378	120.496	
		LYS607:HN - ARG1012:O	1.86996	153.256	
		ILE1014:HN - LYS607:O	1.6008	159.075	
		GLY1178:HN - :UNL1:O	2.15752	152.073	
		LEU1430:HN - LEU1426:O	2.46447	99.622	
		LEU1430:HN - MET1428:O	2.5362	144.884	
		ARG1431:HN - LEU1426:O	1.80307	147.712	
		ARG1431:HE- SP1427:OD1	2.14852	131.092	

		ARG1431:HH21-LN1423:OE1	1.61975	140.23	
		THR1434:HG1- ASP1404:OD1	2.46207	130.404	
		GLY1435:HN - SER1401:O	2.3088	162.207	
		GLY1435:HN - ASP1402:O	2.85862	113.014	
		LEU1436:HN - ASP1402:O	2.27033	156.936	
		UNL1:H - MET622:O	2.49982	94.362	
		UNL1:H - GLY623:O	1.99832	130.163	
2	-7.39	ARG517:HE - GLU1017:OE2	2.43747	122.335	6B
		ARG1012:HN1 - GLN605:O	2.26039	123.973	
		ILE1014:HN - LYS607:O	2.56727	141.03	
		ARG1092:HH12 - :UNL1:O	2.30232	142.977	
		GLN1267:HE22 - :UNL1:O	2.74624	113.044	
		LEU1430:HN - LEU1426:O	2.96046	106.893	
		LEU1430:HN - MET1428:O	2.4405	139.718	
		ARG1431:HN - LEU1426:O	2.07249	153.717	
		GLY1435:HN - SER1401:O	2.33415	135.765	
		LEU1436:HN - ASP1402:O	1.77206	151.67	
		ARG1438:HH2- ARG1399:O	2.4378	120.496	
		LYS607:HN - ARG1012:O	1.86996	153.256	
		ILE1014:HN - LYS607:O	1.6008	159.075	
		LEU1430:HN - LEU1426:O	2.46447	99.622	
		LEU1430:HN - MET1428:O	2.5362	144.884	
		ARG1431:HN - LEU1426:O	1.80307	147.712	
		ARG1431:HE - ASP1427:OD1	2.14852	131.092	
		ARG1431:HH21- LN1423:OE1	1.61975	140.23	
		THR1434:HG1- ASP1404:OD1	2.46207	130.404	
		GLY1435:HN - SER1401:O	2.3088	162.207	
		GLY1435:HN - ASP1402:O	2.85862	113.014	
		LEU1436:HN - ASP1402:O	2.27033	156.936	
		:UNL1:H - SER1098:OG	2.21543	141.836	
3	-7.06	ARG517:HE - GLU1017:OE2	2.43747	122.335	6C
		ARG1012:HN - GLN605:O	2.54359	106.595	
		ILE1014:HN - LYS607:O	2.56727	141.03	
		LEU1430:HN - LEU1426:O	2.96046	106.893	
		LEU1430:HN - MET1428:O	2.4405	139.718	
		ARG1431:HN - LEU1426:O	2.07249	153.717	
		GLY1435:HN - SER1401:O	2.33415	135.765	
		LEU1436:HN - ASP1402:O	1.77206	151.67	
		ARG1438:HH21- ARG1399:O	2.4378	120.496	
		LYS607:HN - ARG1012:O	1.86996	153.256	
		ILE1014:HN - LYS607:O	1.6008	159.075	
		LEU1430:HN - LEU1426:O	2.46447	99.622	
		LEU1430:HN - MET1428:O	2.5362	144.884	
		ARG1431:HN - LEU1426:O	1.80307	147.712	
		ARG1431:HE - ASP1427:OD1	2.14852	131.092	
		ARG1431:HH21- LN1423:OE1	1.61975	140.23	
		THR1434:HG1- ASP1404:OD1	2.46207	130.404	
		GLY1435:HN - SER1401:O	2.3088	162.207	
		GLY1435:HN - ASP1402:O	2.85862	113.014	
		LEU1436:HN - ASP1402:O	2.27033	156.936	
		:UNL1:H - PHE1097:O	1.80964	133.492	
		ARG517:HE - GLU1017:OE2	2.43747	122.335	6D

		ARG1012:HN - GLN605:O	2.54359	106.595
4	-3.82	ILE1014:HN - LYS607:O	2.56727	141.03
		LEU1430:HN - LEU1426:O	2.96046	106.893
		LEU1430:HN - MET1428:O	2.4405	139.718
		ARG1431:HN - LEU1426:O	2.07249	153.717
		GLY1435:HN - SER1401:O	2.33415	135.765
		LEU1436:HN - ASP1402:O	1.77206	151.67
		ARG1438:HH21- ARG1399:O	2.4378	120.496
		ARG468:HH22 - :UNL1:O	2.78895	136.475
		LYS607:HN - ARG1012:O	1.86996	153.256
		ILE1014:HN - LYS607:O	1.6008	159.075
		LEU1430:HN - LEU1426:O	2.46447	99.622
		LEU1430:HN - MET1428:O	2.5362	144.884
		ARG1431:HN - LEU1426:O	1.80307	147.712
		ARG1431:HE - ASP1427:OD1	2.14852	131.092
		ARG1431:HH21- LN1423:OE1	1.61975	140.23
		THR1434:HG1- ASP1404:OD1	2.46207	130.404
		GLY1435:HN - SER1401:O	2.3088	162.207
		GLY1435:HN - ASP1402:O	2.85862	113.014
		LEU1436:HN - ASP1402:O	2.27033	156.936
		:UNL1:H - ARG526:O	1.84116	145.453
		:UNL1:H - ASP615:OD2	2.08867	121.955
		:UNL1:H - ARG526:O	2.12539	97.49
		:UNL1:H - ARG526:O	2.1354	97.011
		:UNL1:H - ALA467:O	1.76668	173.993

Using AutoDock4.2, the lowest binding energy docked conformation of antibacterial compounds 1, 2, 3, and 4 with DNA gyrase receptor was found to be -7.09 kcal/mol, -7.39 kcal/mol, -7.06 kcal/mol, and -3.82 kcal/mol, respectively. These findings provide insight into the putative binding mode and interactions of various potent anti-bacterial and anti-fungal compounds against the DNA gyrase receptor[24]. The results of the docking analysis indicate that compounds that target bacteria prefer to bind at the position at which the DNA double-helical strand binds (Figures 4 and 5A–5D). This suggests that the compounds may prevent the DNA strand from attaching and so have antibacterial properties. Next, residues involved in the binding of the aforementioned antibacterial medication compounds are investigated by Van der Waals and electrostatic interaction analysis. Additionally, as demonstrated in Figures 6A–6D, the molecular docking analysis of DNA gyrase and drug complexes reveals the hydrogen bonding interaction in addition to other non-bonded interactions like van der Waals, carbon–hydrogen bonding, alkyl, pi–alkyl, pi–carbon, and pi–pi–t-shaped type interactions[25]. As Figures 6A–6D and Table-3 demonstrate, every docked complex is stabilized by the standard carbon–hydrogen and van der Waals interaction type. While the alkyl and pi-alkyl types of non-bonded interactions are displayed in Figure 6A, the pi-pi T-shaped and pi-alkyl types of interactions are displayed in Figure 6B by the DNA gyrase and compound 2, the pi-pi t-shaped and pi-alkyl types of interactions are displayed in Figure 6C by the DNA gyrase and compound 3, and the pi-pi t-shaped and pi-alkyl non-bonded interactions are displayed in Figure 6D by the DNA gyrase and compound 4. With the help of bound and non-bonded interactions, the isolated drug compounds stabilize and form a stable complex with the DNA gyrase, as our docking investigation demonstrates[26-29]. This could further restrict DNA gyrase activity, preventing the changes in DNA topology that are catalyzed and causing cell apoptosis, which ultimately results in cell death[30-32].

4. Conclusion

In summary, this study's results indicate that four compounds have been obtained from *B. Cunicularis* tissue. These compounds were identified using mass spectral, UV, FT-IR, and NMR data. Biological analysis of the extracted compounds indicated that all four compounds exhibited strong antibacterial activity. Docking simulation-derived binding orientation and energy data indicated that compounds 1, 2, and 3 had lower binding energies than compound 4. These results could potentially explain the tissue's potential medical applications. Nevertheless, none of the four isolated compounds are ideal for use as drugs.

Acknowledgments

The authors remain grateful to Dr. V. R. Patil, Principle, Rani Laxmibai Mahavidyalay Parola, Jalgaon for their consistent encouragement and support during this work. Acknowledges the vice chancellor of KBCNMU Jalgaon for financial support under the vice chancellor research motivation scheme.

ORCID
Sanjay Chavan:0000-0002-4281-7815
Anil G. Beldar:0000-0002-8452-2468
Rekha B. More: 0000-0002-3765-7466

References

[1] Li Y.; Liu Y.B.; Yu S.S. Grayanoids from the Ericaceae family: structures, biological activities and mechanism of action. *Phytochem. Rev.* **2013**, *12*, 305-325.
[2] Wu H.F.; Morris-Natschke S.L.; Xu X.D.; Yang M.H.; Cheng Y.Y.; Yu S.S.; Lee K.H. Recent advances in natural anti-HIV triterpenoids and analogs. *Med. Res. Rev.* **2020**, *40*, 2339-2385.
[3] Guo B.J.; Liu Z.; Ding M.Y.; Li F.; Jing M.; Xu L.P.; Wang Y.Q.; Zhang Z.J.; Wang Y.; Wang D.; Zhou G.C. Andrographolide derivative ameliorates dextran sulfate sodium-induced experimental colitis in mice. *Biochem. Pharmacol.* **2019**, *163*, 416-424.
[4] Chavan S.V.; Patil A.A.; Rajput S.S.; Borale R.P.; Dhivare R.S. Extraction and analysis of bioactive compound from freshwater crab tissue. In *AIP Conf. Proc.* **2021**, *2369*, 020031.
[5] Xiao Y.; Yuan P.; Sun Y.; Xu Y.; Deng X.; Wang X.; Liu R.; Chen Q.; Jiang L. Comparison of topical antifungal agents for oral candidiasis treatment: a systematic review and meta-analysis. *Oral Surg. Oral Med. Oral Pathol. Oral Radiol.* **2022**, *133*, 282-291.
[6] Elkhawas Y.A.; Ewida M.A.; Ewida H.A.; Gonaid M.; Khalil N. Antiproliferative and apoptotic activities of tomato bioactive metabolite on MDA-MB-435 cell line: in silico molecular modeling and molecular dynamics investigation. *Future J. Pharm. Sci.* **2023**, *9*, 87.
[7] Mohanvel S.K.; Ravichandran V.; Kamalanathan C.; Satish A.S.; Ramesh S.; Lee J.; Rajasekharan S.K. Molecular docking and biological evaluation of novel urea-tailed mannich base against Pseudomonas aeruginosa. *Microb. Pathog.* **2019**, *130*, 104-111.
[8] Shankar Panda B.; Samanta B.; Sudha Ambadipudi S.S.; Nayak S.; Lakshma Nayak V.; Ramakrishna S.; Mohapatra S.; Mohan Behera P.; Samanta L. New 2H-Chromene-Based Hydrazone Derivatives as Promising Anti-Breast Cancer Agents: Efficient Synthesis, Spectral Characterization, Molecular Docking, and ADMET Studies. *ChemistrySelect* **2024**, *9*, e202400115.
[9] Linciano P.; Cavalloro V.; Martino E.; Kirchmair J.; Listro R.; Rossi D.; Collina S. Tackling antimicrobial resistance with small molecules targeting LsrK: Challenges and opportunities. *J. Med. Chem.* **2020**, *63*, 15243-15257.

[10] Tiwari P.; Khare T.; Shriram V.; Bae H.; Kumar V. Plant synthetic biology for producing potent phyto-antimicrobials to combat antimicrobial resistance. *Biotechnol. Adv.* **2021**, *48*, 107729.
[11] Chavan S.V. Study of natural products from freshwater biodiversity is recent strategy: An overview. *World J. Pharm. Res.* **2022**, *11*, 395-418.
[12] Moreno Cardenas C.; Çiçek S.S. Structure-dependent activity of plant natural products against methicillin-resistant Staphylococcus aureus. *Front. Microbiol.* **2023**, *14*, 1234115.
[13] Vikram A. Citrus bioactive compounds: Isolation, characterization and modulation of bacterial intercellular communication and virulence (Doctoral dissertation, Texas A&M University).
[14] Boman H.G. Peptide antibiotics and their role in innate immunity. *Annu. Rev. Immunol.* **1995**, *13*, 61-92.
[15] Warshaviak D.T.; Golan G.; Borrelli K.W.; Zhu K.; Kalid O. Structure-Based Virtual Screening Approach for Discovery of Covalently Bound Ligands. *J. Chem. Inf. Model.* **2014**, *54*, 1941-1950.
[16] ZINC Database. Available online: https://zinc15.docking.org (accessed on [insert date]).
[17] Vistoli G.; Pedretti A.; Testa B. Assessing drug-likeness–what are we missing? *Drug Discov. Today* **2008**, *13*, 285-294.
[18] Lipinski C.A.; Lombardo F.; Dominy B.W.; Feeney P.J. Experimental and computational approaches to estimate solubility and permeability in drug discovery and development settings. *Adv. Drug Deliv. Rev.* **1997**, *23*, 3-25.
[19] Singh D.B.; Gupta M.K.; Singh D.V.; Singh S.K.; Misra K. Docking and in silico ADMET studies of noraristeromycin, curcumin and its derivatives with Plasmodium falciparum SAH hydrolase: a molecular drug target against malaria. *Interdiscip. Sci. Comput. Life Sci.* **2013**, *5*, 1-2.
[20] Daina A.; Michielin O.; Zoete V. SwissADME: a free web tool to evaluate pharmacokinetics, drug-likeness and medicinal chemistry friendliness of small molecules. *Sci. Rep.* **2017**, *7*, 42717.
[21] Bhal S.K.; Kassam K.; Peirson I.G.; Pearl G.M. The rule of five revisited: applying log D in place of log P in drug-likeness filters. *Mol. Pharm.* **2007**, *4*, 556-560.
[22] Bickerton G.R.; Paolini G.V.; Besnard J.; Muresan S.; Hopkins A.L. Quantifying the chemical beauty of drugs. *Nat. Chem.* **2012**, *4*, 90-98.
[23] BIOVIA DS. BIOVIA workbook, release 2017; BIOVIA pipeline pilot, release 2017. *San Diego: Dassault Systèmes* **2020**.
[24] Hassan A.S.; Askar A.A.; Naglah A.M.; Almehizia A.A.; Ragab A. Discovery of new Schiff bases tethered pyrazole moiety: Design, synthesis, biological evaluation, and molecular docking study as dual targeting DHFR/DNA gyrase inhibitors with immunomodulatory activity. *Molecules* **2020**, *25*, 2593.
[25] Sugar A.M.; Liu X.P.; Chen R.J. Effectiveness of quinolone antibiotics in modulating the effects of antifungal drugs. *Antimicrob. Agents Chemother.* **1997**, *41*, 2518-2521.
[26] Zaghary W.A.; Anwar M.M.; El-Karim A.; Somaia S.; Awad G.E.; Hussein G.K.; Mahfouz N.M. Design, Synthesis and Molecular Docking of New Benzimidazole Derivatives of Potential Antimicrobial Activity as DNA Gyrase and Topoisomerase IV Inhibitors. *Egypt. J. Chem.* **2021**, *64*, 3817-3839.
[27] Porollo A.; Meller J. Polyview-M.M.: web-based platform for animation and analysis of molecular simulations. *Nucleic Acids Res.* **2010**, *38*, W662-W666.
[28] Chavan S. Aquatic natural product chemistry. *LAMBERT Academic Publishing* **2024**, ISBN: 978-620-7-45057-2.
[29] Kumbhar B.V.; Borogaon A.; Panda D.; Kunwar A. Exploring the origin of differential binding affinities of human tubulin isotypes αβII, αβIII and αβIV for DAMA-colchicine using homology modelling, molecular docking and molecular dynamics simulations. *PLoS One* **2016**, *11*, e0156048.
[30] Rai A.; Gupta T.K.; Kini S.; Kunwar A.; Surolia A.; Panda D. CXI-benzo-84 reversibly binds to tubulin at colchicine site and induces apoptosis in cancer cells. *Biochem. Pharmacol.* **2013**, *86*, 378-391.
[31] Venghateri J.B.; Gupta T.K.; Verma P.J.; Kunwar A.; Panda D. Ansamitocin P3 depolymerizes microtubules and induces apoptosis by binding to tubulin at the vinblastine site. *PLoS One* **2013**, *8*, e75182.
[32] Waterhouse A.; Bertoni M.; Bienert S.; Studer G.; Tauriello G.; Gumienny R.; Heer F.T.; de Beer T.A.; Rempfer C.; Bordoli L.; Lepore R. SWISS-MODEL: homology modelling of protein structures and complexes.